[CANCER RESEARCH 64, 5850–5860, August 15, 2004]

Synergistic Activation of Innate Immunity by Double-Stranded RNA and CpG DNA Promotes Enhanced Antitumor Activity

Mark M. Whitmore,[1] Michael J. DeVeer,[4] Andrea Edling,[2] Rhonda K. Oates,[3] Brenna Simons,[1] Daniel Lindner,[1,3] and Bryan R. G. Williams[1]

Departments of [1]Cancer Biology and [2]Immunology, Lerner Research Institute and [3]Center for Drug Discovery and Development, Taussig Cancer Center, The Cleveland Clinic Foundation, Cleveland, Ohio, and [4]Center for Animal Biotechnology, Melbourne University, Parkville, Victoria, Australia

ABSTRACT

Double-stranded RNA (dsRNA) and unmethylated CpG sequences in DNA are pathogen-associated molecular patterns of viruses and bacteria that activate innate immunity. To examine whether dsRNA and CpG DNA could combine to provide enhanced stimulation of innate immune cells, murine macrophages were stimulated with poly-rI:rC (pIC), a dsRNA analog, and CpG-containing oligodeoxynucleotides (CpG-ODN). Combined treatments demonstrated synergy in nitric oxide, interleukin (IL)-12, tumor necrosis factor α, and IL-6 production. Studies using neutralizing antibodies for type I interferons (IFNs), IFN-α and IFN-β, indicated that nitric oxide synthase synergism is mediated by paracrine/autocrine effects of IFN-β. In contrast, enhanced cytokine production occurred independent of type I IFN and was maintained in macrophages from IFN-α/β receptor knockout mice. Cotransfection of human Toll-like receptors 3 and 9 (receptors for dsRNA and CpG DNA, respectively) into 293T cells supported synergistic activation of an IL-8 promoter reporter construct by pIC, indicating interaction of the signaling pathways in driving the synergy response. *In vivo* stimulation of mice with pIC and CpG-ODN demonstrated synergy for serum IL-6 and IL-12p40 levels that correlated with an enhanced antitumor effect against established B16-F_{10} experimental pulmonary metastases. Treatment of tumor-bearing mice with pIC and CpG-ODN in combination resulted in enhanced nitric oxide synthase expression in lung tissue and enhanced up-regulation of class I major histocompatibility complex on splenic dendritic cells relative to treatments with either agent alone. In conclusion, the combined detection of viral pathogen-associated molecular patterns, *i.e.*, dsRNA and CpG DNA, may mimic definitive viral recognition, resulting in an enhanced innate immune response that could be used for tumor vaccination or immunotherapy.

INTRODUCTION

The mammalian innate immune system functions to identify the presence of infection through recognition of macromolecular structures that are characteristic of pathogenic organisms, termed pathogen-associated molecular patterns (PAMPs). Lipopolysaccharide (LPS) and immunostimulatory CpG DNA sequences are PAMPs associated with bacterial and large DNA virus infection, whereas double-stranded RNA (dsRNA), a viral replication intermediate, represents a molecule characteristic of viral infection. A variety of pattern recognition receptors (PRRs) are involved with PAMP identification. These include the Toll-like receptors (TLRs), which are activated by their ligands at the cell surface or in the endosomal/lysosomal compartment (1), and intracellular receptors such as the dsRNA-dependent protein kinase (PKR) and 2′-5′ oligoadenylate synthetases (2). Activated PRRs initiate signaling cascades that regulate the expression of a number of proteins including type I interferons (IFNs), proinflammatory cytokines, and nitric oxide synthase (NOS2; Refs. 3 and 4). Ligation of PRRs also stimulates maturation of dendritic cells (DCs) for antigen presentation. These immune functions not only inhibit pathogen propagation during infection but also support development of acquired immune responses. Indeed, many preclinical studies have demonstrated that PAMP stimulation of the innate immune system is critical for the efficacy of tumor vaccines (5) and immune-based therapies (6, 7).

Based on two disparate observations, we have hypothesized that CpG DNA in combination with dsRNA could provide enhanced stimulation of innate immunity that could lead to an effective tumor immunotherapy. First, in nonclinical studies, dsRNA and CpG DNA are present in one of the most effective vectors for plasmid DNA-based tumor vaccines, *i.e.*, plasmid DNA that encodes the Sindbis virus replicon (pSIN; Refs. 5 and 8). In comparison with conventional cytomegalovirus-based plasmid vectors (pCMV), pSIN can break host tolerance to syngeneic tumors with 2–3 orders of magnitude improved potency (8). A potential explanation for the improved efficacy of pSIN is the greater levels of dsRNA produced by the SIN replicon (8, 9). Indeed, PKR, a dsRNA-responsive serine threonine kinase, is activated during pSIN transfection, and the RNAse L arm of the intracellular dsRNA response is required for optimal development of acquired immunity during pSIN vaccination (5). Because CpG DNA sequences exist in the plasmid component of both pCMV and pSIN vectors (10, 11), it is of interest to determine whether dsRNA and CpG DNA in combination could provide enhanced stimulation of innate immunity in comparison with treatment with either agent alone. Moreover, dsRNA and CpG DNA are present during infection with large DNA viruses. Whereas it is well established that dsRNA is a significant PAMP produced during infection with large DNA viruses (12–15), recent evidence establishes unmethylated CpG DNA as a PAMP for large DNA viruses. Indeed, the CpG dinucleotide frequency in large DNA viruses is similar to that of bacterial DNA (16, 17), and DNA fractions from large DNA viruses such as herpes simplex virus (HSV) and adenovirus can be stimulatory (18, 19). Moreover, TLR9 is required for plasmacytoid DC recognition of HSV (20, 21). Therefore, because CpG DNA and dsRNA are present during pSIN vaccinations as well as large DNA viral infection, we predict that dual recognition of these two PAMPs mimics viral infection, resulting in enhanced activation of the innate immune response.

Double-stranded RNA, which is recognized by TLR3 (22), PKR (23), and 2′-5′ oligoadenylate synthetases (24, 25), and CpG DNA, which is recognized by TLR9 (26, 27), stimulate immune activities that are favorable for inhibiting tumor growth. First, the induction of type 2 NOS2 in macrophages leads to the production of nitric oxide (NO) that possesses bactericidal, virucidal, and tumoricidal activities (4, 28). Proinflammatory cytokines such as interleukin (IL)-12, tumor necrosis factor (TNF)-α, and IL-6 produced in monocytes, macrophages, and DCs can promote development of acquired immunity in part through stimulation of IFN-γ production from natural killer (NK) and T cells and antigen presentation functions (29, 30). Type I IFNs are well known for their antitumor and antiviral effects through their ability to directly inhibit cell growth as well as viral replication (2). Finally, cytolytic activity of NK cells is an important component of

Received 1/9/04; revised 6/5/04; accepted 6/21/04.

Grant support: NIH RO1 AI34039, PO1 CA62220.

The costs of publication of this article were defrayed in part by the payment of page charges. This article must therefore be hereby marked *advertisement* in accordance with 18 U.S.C. Section 1734 solely to indicate this fact.

Requests for reprints: Bryan R. G. Williams, Department of Cancer Biology, NB40 Lerner Research Institute, The Cleveland Clinic Foundation, 9500 Euclid Avenue, Cleveland, OH 44195.

viral defense and many strategies for tumor immune therapy (31, 32). Thus, if dsRNA and CpG DNA combine for enhanced activation of innate immunity, the combination is likely capable of providing improved tumor clearance.

Here we describe for the first time synergism between dsRNA and CpG DNA for the activation of a macrophage-like cell line (RAW 264.7) and primary bone marrow-derived macrophages (BMMs). RAW 264.7 cells or BMMs treated with synthetic mimics of dsRNA and CpG DNA (*i.e.*, pIC and CpG-ODN) resulted in the synergistic induction of NOS2, IL-12p40, TNF-α, and IL-6. Type I IFNs were shown to play a role in mediating the NOS2 response; however, synergism resulting in cytokine production was independent of type I IFNs. In cotransfection studies of non-macrophage 293T cells, synergism was demonstrated between human TLR3 and TLR9 for the activation of IL-8 promoter reporter constructs. These observations were extended *in vivo*, where the combination demonstrated synergism for eliciting IL-6 and IL-12p40 serum levels in mice and provided an enhanced antitumor response to established B16-F_{10} pulmonary metastases in comparison with treatments with pIC or CpG-ODN alone. Finally, treatment with pIC and CpG-ODN *in vivo* stimulated enhancement of NOS2 expression in the lungs and class I major histocompatibility complex expression in splenic DCs.

MATERIALS AND METHODS

Reagents and Mice. The p3XFLAG vector (Sigma, St. Louis, MO), IL-8 luciferase reporter, and the TLR expression plasmids were a kind gift from Dr. J. DiDonato (Lerner Research Institute, Cleveland Clinic, Cleveland, OH). The pRL-TK vector and polyinsosinic:polycytidylic acid were purchased from Sigma. Phosphorothioate CpG and non-CpG oligodeoxynucleotides were purchased from Midland Certified Reagent Co. (Midland, TX) as reverse-phase high-performance liquid chromatography purification grade. All oligodeoxynucleotides were determined to be free of endotoxin ($<$0.1 EU/mg) by the QCL-1000 Chromogenic *Limulus* Amebocyte Lysate Assay from BioWhittaker, Inc. (Walkersville, MD). All primer pairs for reverse transcription-polymerase chain reaction (RT-PCR; sequences are indicated below) were purchased from Invitrogen (Carlsbad, CA) as custom-synthesized oligodeoxynucleotides, except for TNF-α and 18S rRNA, which were purchased from Ambion, Inc. (Austin, TX) as the *TNF-α* gene-specific relative RT-PCR Kit. Neutralizing antibody for mouse IFN-α (MCA 1431) was purchased from Accurate Chemical and Scientific Corp. (Westbury, NY). Neutralizing antibody for mouse IFN-β was purchased from US Biological (Swampscott, MA). The rabbit polyclonal antibody for mouse NOS2 was purchased from Upstate Biotechnology, Inc. (Waltham, MA). The antibodies for flow cytometric analysis were purchased from BD Biosciences-PharMingen (San Diego, CA). Wild-type C57BL/6 and 129SV mice were purchased from Taconic Co. (Germantown, NY). Type I IFN-α/βR-KO mice, isogenic on 129SV, were a kind gift from Dr. Thomas Hamilton (Lerner Research Institute, The Cleveland Clinic Foundation).

Cell Lines and Primary BMMs. Human 293T cells and mouse RAW 264.7, L929, and B16-F_{10} melanoma cells were maintained in culture with Dulbecco's modified Eagle's medium supplemented with 10% fetal bovine serum and antibiotics at 37°C in an atmosphere of 5% CO_2. Bone marrow prepared from the femur of a C57BL/6, 129SV, or type I IFN-α/βR-KO mouse, as indicated, was differentiated in culture for 7–10 days in RPMI 1640 supplemented with 15% fetal bovine serum, 15% L-cell conditioned medium, β-mercaptoethanol, and antibiotics to produce BMMs. L-cell conditioned medium served as the source of murine macrophage colony-stimulating factor.

Cell Stimulations. RAW 264.7 cells or primary macrophages were plated in either 96- or 48-well plates. Two days after plating, growth medium was removed and replaced with fresh growth medium supplemented with the indicated concentrations of either pIC, immunostimulatory CpG phosphorothioate oligodeoxynucleotide 1826 (CpG-ODN 1826), 5′-TCCATGACGTTCCTGACGTT-3′ (33), or non-immunostimulatory CpG phosphorothioate oligodeoxynucleotide 1982, 5′-TCCAGGACTTCTCTCAGGTT-3′ (33), either alone or in combination. In experiments with type I IFN-neutralizing antibodies, the indicated immunostimulatory nucleic acids were added to fresh growth medium supplemented with or without neutralizing antibody at the indicated concentrations. Before the experiment, the titer of neutralizing units for each antibody was determined by the ability to block recombinant IFN-α or -β protection of L929 cells from encephalomyocarditis virus (EMCV) challenge. The mixture was then added to cells plated on a 96-well plate as described above and incubated for 16 or 24 h.

Assays for Nitrite and Cytokine in Culture Supernatants and Mouse Serum. Culture supernatants were collected 6, 16, or 24 h after stimulation and cleared of debris by a brief centrifugation (500 $\times$ *g* for 5 min). Cleared supernatants were either stored at −20°C until the time of assay or immediately assessed for nitrite or cytokine. Nitrite was measured by Griess assay. Culture supernatants were assessed for murine IL-12p40, IL-6, or mouse TNF-α by sandwich enzyme-linked immunosorbent assay (ELISA) using the mouse BD OptEIA ELISA sets (BD Biosciences) following the manufacturer's instructions. Type I IFN was measured by viral protection assays of L929 cells with EMCV as challenging virus.

Reverse Transcription-Polymerase Chain Reaction. On the second day after plating, RAW 264.7 cells or BMMs were stimulated with either medium or the indicated concentrations of pIC and CpG-ODN either alone or in combination. At the indicated time after treatment, medium was removed, and total cellular RNA was isolated using Trizol reagent (Life Technologies, Inc., Grand Island, NY) according to the manufacturer's instructions. Total RNA was reverse transcribed into cDNA using poly(A) priming and Superscript II (Life Technologies, Inc.) reverse transcriptase according to the manufacturer's instructions. The cDNA was then amplified by two-temperature (95°C for 15 s and 60°C for 1 min) PCR for 25–30 cycles using PlatinumTaq (Life Technologies, Inc.) and primers specific for *NOS2*, *IL-12p40*, *IL-6*, and *TNF-α*. The *NOS2*, *IL-12p40*, and *IL-6* PCR primers were selected from the work of Overbergh *et al.* (34), and the sequences were as follows: *NOS2* forward primer, 5′-CAG-CTG-GGC-TGT-ACA-AAC-CTT-3′; *NOS2* reverse primer, 5′-CAT-TGG-AAG-TGA-AGC-GTT-TCG-3′; *IL-12p40* forward primer, 5′-GGA-AGC-ACG-GCA-GCA-GAA-TA-3′; *IL12p40* reverse primer, 5′-AAC-TTG-AGG-GAG-AAG-TAG-GAA-TGG-3′; *IL-6* forward primer, 5′-CAG-AAT-TGC-CAT-CGT-ACA-ACT-CTT-TTC-TCA-3′; and *IL-6* reverse primer, 5′-AAG-TGC-ATC-ATC-GTT-GTT-CAT-ACA-3′. Murine *TNF-α* was measured using the *TNF-α* gene-specific relative RT-PCR Kit from Ambion, Inc. The PCR for *IFN-β* was performed as described above, except that a temperature cycle of 95°C for 30 s, 55°C for 30 s, and 72°C for 1 min and 45 s for 40 cycles was used. The PCR primers specific for *IFN-β* were selected from the work of Toshchakov *et al.* (35), and the sequences were as follows: *IFN-β* forward primer, 5′-TCC-AAG-AAA-GGA-CGA-ACA-TTC-G-3′; *IFN-β* reverse primer; and 5′-TGA-GGA-CAT-CTC-CCA-CGT-CAA-3′. PCR products were separated on a 2% agarose/Tris-acetate EDTA gel and stained with ethidium bromide for visualization. All RT-PCR reactions gave single products.

Quantitative real-time PCR for murine *IFN-β* and glyceraldehyde-3-phosphate dehydrogenase (GAPDH) as a housekeeping control was performed on cDNA samples prepared from treated cells as described above using Ω Beacon Gene Expression Sets from Gorilla Genomics, Inc. (Alameda, CA) according to the manufacturer's instructions. The temperature cycle was 95°C for 30 s, 55°C for 30 s, and 72°C for 30 s for 45 cycles. The cross-threshold cycle (C_t) was measured using an iCycler and associated software from Bio-Rad (Hercules, CA). Copy number was determined from a standard curve of C_t *versus* copy number using cDNA standards for either *IFN-β* or *GAPDH*. Relative copy number was calculated as *IFN-β* copy number/*GAPDH* copy number. Real-time PCR analysis for *NOS2*, *IL-12p40*, and *TNF-α* was performed using SYBR-Green (Perkin-Elmer) according to the manufacturer's instructions with the specific primer pairs indicated above and primer pairs for 18S rRNA as reference RNA (Classic 18S primer pairs; Ambion, Inc.). The two-temperature cycle of 95°C for 15 s and 60°C for 1 min (repeated for 40−45 cycles) was used, and Ct was measured using the iCycler. Relative transcript quantities were calculated by the Δ-ΔCt method using 18S rRNA as a reference amplified from samples using the Classic 18S primer pairs from Ambion, Inc. Normalized samples were then expressed relative to the average ΔCt value for untreated controls to obtain relative fold change in expression levels.

Transfections and Luciferase Assay. All transfections were performed in 293T cells using LipofectAMINE 2000 (Invitrogen) according to the manufacturer's instructions. The amounts of DNA were 50 ng of TLR expression

vector, 25 ng of luciferase reporter vector, and 10 ng of pRL-TK made up to 725 ng with p3XFLAG. At 24 h after transfection, cells were plated evenly onto a 96-well plate. At 36 h after transfection, pIC was added for 8–16 h. The cells were then lysed and assayed according to the Promega Dual Luciferase Assay Protocol (Promega). Luminescence was recorded on a Lumistar Galaxy luminometer (BMG Lab Technologies). All results were standardized using renilla luciferase activity. All assays were performed at least three times, and results were representative.

***In Vivo* Assessment of Serum Cytokine Levels.** C57BL/6 mice received intraperitoneal injection with phosphate-buffered saline (PBS), pIC (30 μg/mouse), CpG-ODN 1826 (20 μg/mouse), or pIC and CpG-ODN 1826 combination at their respective doses in a total injection volume of 200 μl. The selected doses were based on preliminary dose-response analyses for intraperitoneal treatments with pIC or CpG-ODN alone and were at or near the ED_{50} (50% effective dose) for each agent (data not shown). Four hours after injection, *i.e.*, the time of peak IL-12 and IL-6 serum levels based on previous studies of CpG-ODN (6, 36), blood was collected by retro-orbital bleed under Avertin anesthesia. Blood was allowed to coagulate for 2 h at room temperature, and serum was isolated as the supernatant after centrifugation for 15 min at 800 $\times$ *g*. Serum was stored at -20°C until the time of assay. IL-12p40 and IL-6 were determined by ELISA as described above.

B16-F_{10} Experimental Pulmonary Metastasis. C57BL/6 mice were inoculated with 1.0×10^5 B16-F_{10} cells in 0.2 ml of Hanks' buffer by tail vein injection on day 0. On day 3 after tumor inoculations, mice were treated with either PBS, pIC (30 μg/mouse), CpG-ODN 1826 (20 μg/mouse), or the combination of pIC and CpG-ODN 1826 by intraperitoneal injection. On day 17 after tumor inoculations, mice were sacrificed by CO_2 asphyxiation and weighed in grams to determine body weight. Lungs were excised and then inflated and fixed in 10% formalin/PBS. Tumor burden was determined by counting black nodules using a dissecting microscope. Tumor-bearing lungs were weighed in grams, and lung tumor mass was determined as the percentage of body mass of tumor-bearing lung minus the average percentage of body mass of tumor-free lungs, *i.e.*, lung tumor mass = [(tumor-bearing lung weight/body weight) $\times$ 100] – mean[(tumor-free lung weight/body weight) $\times$ 100]. The mean percentage of body mass for tumor free lungs was 1.2% (g/g).

NOS2 Expression in Lungs. Mice were inoculated with tumor and treated on day 3 after inoculation with PBS, pIC alone, CpG alone, or pIC and CpG in combination as described above. Twenty-four hours after treatment, lungs were excised from mice and flash-frozen in liquid N_2. Lungs were then homogenized on ice in 1 ml of lysis buffer [50 mM Tris-HCl (pH 7.6), 1% Nonidet P-40, 150 mM NaCl, 5 mM EDTA, 100 mM NaF, 2 mM Na PP_i, 2 mM sodium orthovanadate, 1 mM dithiothreitol, 10% glycerol, 1 mM phenylmethylsulfonyl fluoride, 10 μg/ml leupeptin, 10 μg/ml pepstatin A, and 10 μg/ml aprotinin] using a Dounce homogenizer. Lung homogenates were then sonicated three times using a bath sonicator. Lung whole cell extracts were cleared of debris by centrifugation (12,000 $\times$ g for 20 min at 4°C). Eighty micrograms of cleared lung lysates were separated on an 8% SDS-polyacrylamide gel electrophoresis gel and transferred to polyvinylidene difluoride membrane. Membranes were probed for NOS2 expression using a rabbit polyclonal antibody specific for mouse NOS2 (Upstate Biotechnology, Inc.) and for β-actin as a loading control by Western blot using appropriate horseradish peroxidase-coupled secondary antibodies. Bands were detected using enhanced chemiluminescence.

Flow Cytometric Analysis of Antigen Presentation Markers in Splenic Dendritic Cells. Mice were inoculated with tumor and treated on day 3 after inoculation with PBS, pIC alone, CpG alone, or pIC and CpG in combination as described above. Twenty-four hours after treatment, spleens were excised from mice, and a single-cell suspension, pooled from two mice, was prepared by pressing spleens though a 70 μm nylon mesh. Contaminating red blood cells were removed by ammonium chloride lysis. The resulting crude splenocytes were stained for two-color analysis using a biotinylated anti-CD11c antibody and fluorescein isothiocyanate-coupled antibodies for class I major histocompatibility complex (MHC), class II MHC, or CD80 purchased from BD Biosciences-PharMingen according to the manufacturer's instructions using Fc block to prevent nonspecific binding of antibodies to the Fc receptor. Cell suspensions were then incubated with phycoerythrin-coupled streptavidin for detection of the biotinylated anti-CD11c antibody. All samples were also stained with appropriate isotype control antibodies for CD11c as well as the antibodies with direct fluorophore couple. Stained samples were fixed in 1% paraformaldehyde/PBS and stored in the dark at 4°C. Within 2 days of staining, surface markers were detected by flow cytometric analysis using a FACScan flow cytometer from Becton Dickinson (San Jose, CA) and analyzed using the associated CELLQuest software from Becton Dickinson. Staining with isotype controls was $<1\%$ in regions where antigen presentation markers were considered positive and did not change with treatment. Presented is a single-color histogram of the indicated antibody gated on CD11c-positive cells, which ranged from 7% to 10% of the total spleen population.

Statistical Analyses and Determination of Synergism. Synergism in concentration-response curves at fixed concentration ratios was determined using

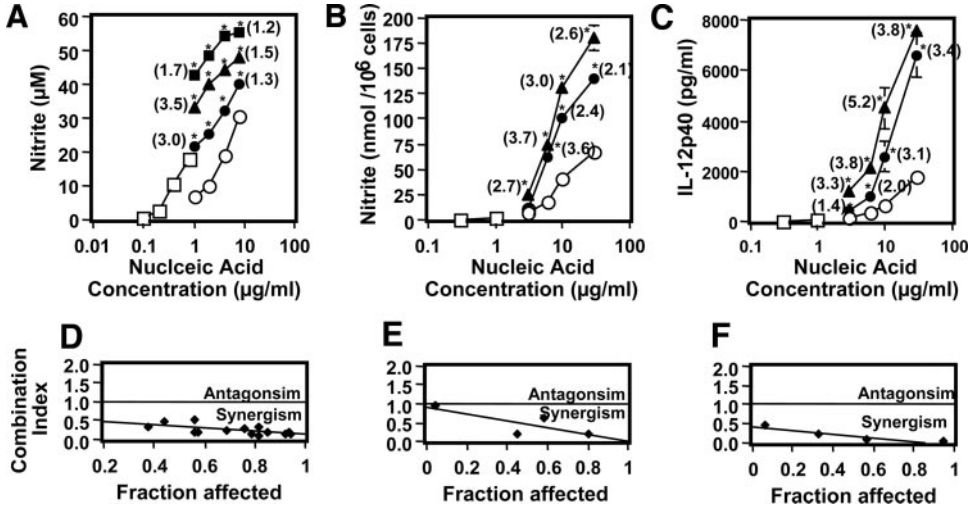

Fig. 1. Synergy between pIC and CpG-ODN for stimulating NO (*A* and *B*) and IL-12p40 (*C*) production in murine macrophages. *A*, NO production by RAW 264.7 cells after 20 h of treatment with CpG-ODN alone (□), pIC alone (○), or varied pIC with constant concentrations of CpG-ODN [*i.e.*, 0.1 μg/ml CpG-ODN (●), 0.2 μg/ml CpG-ODN (▲), or 0.8 μg/ml CpG-ODN (■)]. *B*, NO production by primary BMMs after 24 h of treatment with CpG-ODN alone (□), pIC alone (○), or varied pIC with constant concentrations of CpG-ODN [*i.e.*, 0.3 μg/ml CpG-ODN (●) and 1 μg/ml CpG-ODN (▲)]. *C*, IL-12p40 production by primary BMMs after 24 h of treatment with CpG-ODN alone (□), pIC alone (○), or varied pIC with constant concentrations of CpG-ODN [*i.e.*, 0.3 μg/ml CpG-ODN (●) or 1 μg/ml CpG-ODN (▲)]. *D*, median effect analysis of drug interaction to determine synergism for NO response in RAW 264.7 cells (*A*). *E*, median effect analysis of drug interaction to determine synergism for NO response in BMMs (*B*). *F*, median effect analysis of drug interaction to determine synergism for IL-12p40 response in BMMs (*C*). In *A* and *B*, NO was determined by assessing culture supernatants for nitrite by the Griess assay. In *C*, IL-12p40 produced in the culture supernatants was determined by ELISA. All data points represent mean ± SE (n = 3–6). *Numbers in parentheses* represent fold synergy, *i.e.*, the fold increase for the combined treatment relative to the sum of the levels observed for each component treated alone. *Stars* represent significant ($P < 0.02$) interaction as determined by two-way ANOVA.

median effect analysis according to Chou and Talalay (37). For single concentration combinations, significant synergism was assessed by two-way analysis of variance (ANOVA; Ref. 38). Student's *t* test was used to evaluate the effects of neutralizing antibodies on similarly treated samples in the absence or presence of neutralizing antibodies. Student's *t* test was also used to determine differences between the indicated treatments for tumor burden and tumor mass.

RESULTS

Synergistic Activation of NOS2 and Proinflammatory Cytokines in Murine Macrophages. To test the hypothesis that dsRNA and CpG DNA could combine to provide enhanced immunostimulation, activation of cultured murine macrophages was measured after treatments with pIC, a synthetic mimic of dsRNA, and CpG-ODN 1826, a synthetic mimic of bacterial DNA, either alone or in simultaneous combination (Fig. 1). Activation was assessed by the release of NO and IL-12p40 into culture supernatants after treatment as measured using the Griess and ELISA assays, respectively. In RAW 264.7 cells, a murine macrophage-like cell line, treatment with either pIC or CpG DNA alone provided the expected concentration-response curves for NO production (Fig. 1*A*). Interestingly, when treated in combination, CpG DNA caused a concentration-dependent enhancement of the NO response to pIC. Indeed, median effect analysis for drug interaction indicated that the combined effects of pIC and CpG DNA were synergistic (Fig. 1*D*). The fold increase in NO ranged from 1.2- to 3.6-fold greater than the additive levels observed using the individual PAMPs ($P < 0.02$). To eliminate immortalization artifacts possible in the RAW 264.7 cells, NO production was measured in primary BMMs from C57BL/6 mice (Fig. 1*B*). The concentration-response to pIC alone was similar that observed with RAW 264.7 cells; however, there was only marginal stimulation of NO production by CpG DNA alone at concentrations up to 1 μg/ml. Most importantly, combined treatment of primary BMMs stimulated concentration-dependent synergism for the NO response (Fig. 1, *B* and *E*). The levels of synergy ranged from 2.1- to 3.7-fold greater than additive levels ($P < 0.02$). When activation was measured by IL-12p40 release from primary BMMs (Fig. 1*C*), a concentration-dependent and synergistic (Fig. 1*F*) response was observed under the condition of combined stimulation, with levels of synergy that ranged from 1.4- to 5.2-fold greater than the additive effects of pIC or CpG alone ($P < 0.02$). Indeed, synergy for both NO and IL-12p40 was CpG-dependent because non-CpG DNA failed to stimulate an enhanced response (data not shown). The optimal concentration ratio (in μg/m) of pIC and CpG for stimulating a synergistic response was 10:1, respectively.

In the sequence of gene induction that follows PAMP stimulation as well as bacterial or viral infection, *IL-12p40* and *NOS2* represent intermediate and late response genes that may be influenced by secondary effects of cytokines or IFNs produced in culture. Thus, we decided measure the early response gene *TNF-α* and the intermediate response gene *IL-6*, which are generally regulated independent from type I IFNs. Indeed, combined stimulation of RAW 264.7 cells with pIC and CpG-ODN resulted in a potentiated IL-6 response (Fig. 2*A*). Similar to NOS2 and IL-12p40, the TNF-α response was synergistic (Fig. 2, *B* and *C*). In data not shown, pIC and CpG-ODN stimulation combined to provide synergistic TNF-α and IL-6 responses in primary BMMs. Finally, synergism was CpG-dependent in both RAW 264.7 cells and primary BMMs because non-CpG-ODN failed to elicit enhanced TNF-α and IL-6 responses (data not shown).

Type I IFN-Dependent and -Independent Mechanisms Mediate the Synergy Response to pIC and CpG DNA. Previous studies have demonstrated that type I IFNs (IFN-α and IFN-β) are capable of enhancing the activation of macrophages by LPS (35, 39). In addition,

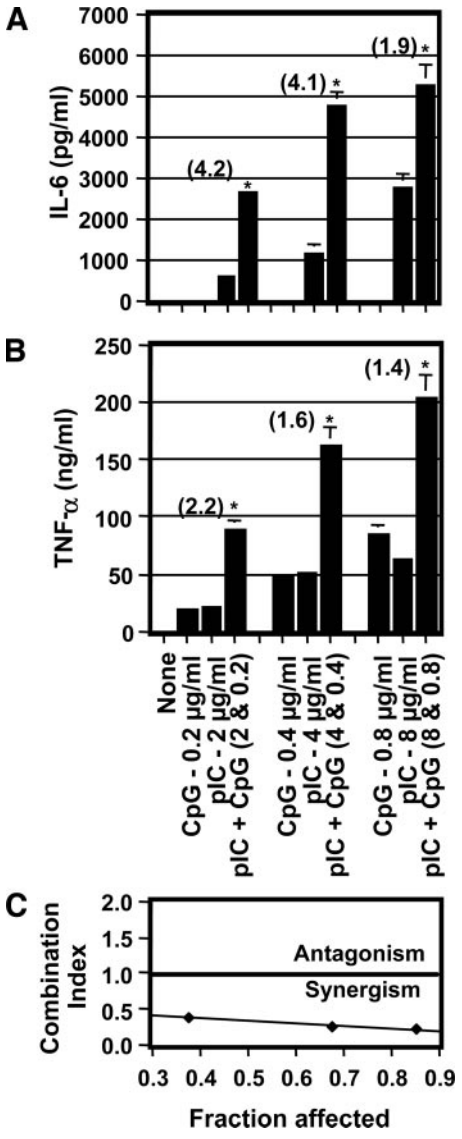

Fig. 2. Synergy between pIC and CpG-ODN for stimulating IL-6 (*A*) and TNF-α (*B* and *C*) in RAW 264.7 cells. IL-6 (*A*) or TNF-α (*B*) was produced by RAW 264.7 cells after 6 h of treatment with CpG-ODN alone, pIC alone, or pIC and CpG-ODN in combination at the indicated concentrations. *C*, median effect analysis of drug interaction for TNF-α response to pIC and CpG-ODN treatment in *B*. IL-6 and TNF-α produced in the culture supernatants were determined by ELISA. All *bars* represent mean ± SE ($n = 6$) of data pooled from two independent experiments. *Numbers in parentheses* represent the fold increase in levels for the combined treatment relative to the sum of the levels observed for each component treated alone. *Stars* represent significant ($P \leq 0.03$) interaction as determined by two-way ANOVA.

our recent studies[4] suggest that type I IFNs may up-regulate TLRs as well as components of TLR signaling pathways. Indeed, all of the genes examined thus for synergism possesses nuclear factor (NF)-κB and activator protein (AP)-1 regulatory elements in their promoter that are regulated by TLR signaling pathways. Because pIC is a strong inducer of type I IFN (40, 41), we decided to measure the role of type I IFNs in regulating pIC and CpG synergism. First, RT-PCR was used to measure the kinetics of proinflammatory gene induction for genes that either possess (*NOS2*) or lack (*TNF-α*, *IL-12p40*, and *IL-6*) IFN-stimulated response elements (ISREs) in their promoter (Fig. 3*A*). As expected, *NOS2*, *IL12p40*, *TNF-α*, and *IL-6* gene induction was strongest, as indicated by scanning densitometry (data not shown), with combined treatment consistent with the enzymatic and

[4] Unpublished observations.

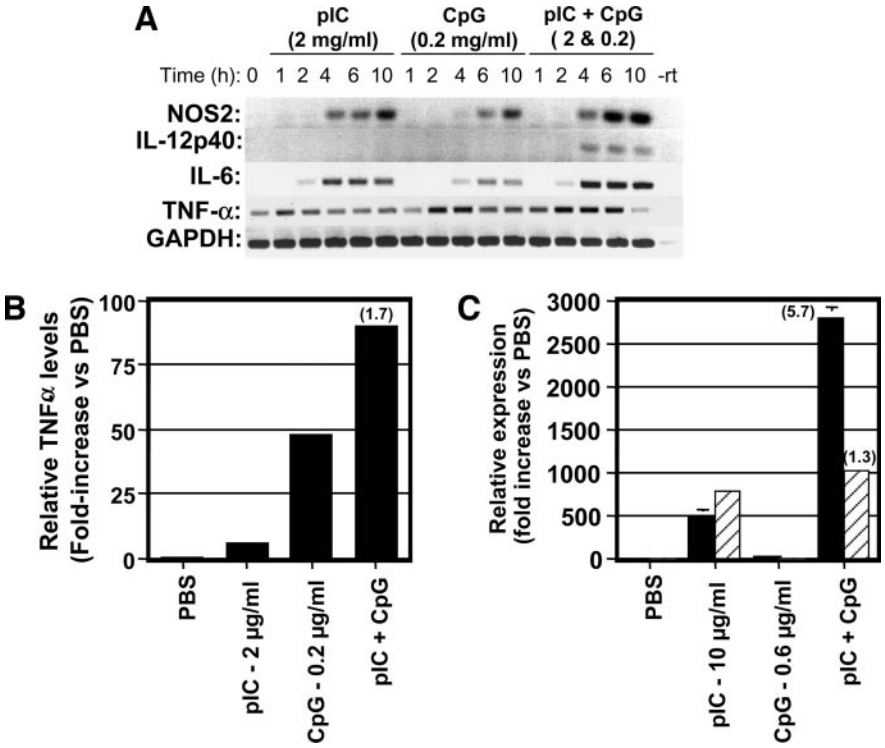

Fig. 3. Gene induction in murine macrophages stimulated with pIC and CpG-ODN. *A*, kinetics of induction for proinflammatory genes that lack (*TNF-α*, *IL-6*, and *IL-12p40*) or possess ISRE control elements (*NOS2*) in their promoter. RT-PCR analysis of cDNA samples prepared at the indicated time after stimulation of RAW 264.7 cells with pIC, CpG, or the combination as indicated. Displayed is a negative image of a 2% agarose gel stained with ethidium bromide. *B*, quantitative real-time PCR analysis for *TNF-α* transcript levels in 4 h cDNA samples of the RAW 264.7 cells treated as described in *A*. The PCR products were amplified using primer pairs specific for *TNF-α* and detected using SYBR-Green. *C*, relative expression of *IL-12p40* (■) and *NOS2* (▨) in primary BMMs stimulated for 6 h with the indicated concentrations of pIC and CpG-ODN alone and in combination. The PCR products were amplified using primer pairs specific for either *IL-12p40* or *NOS2* and detected using SYBR-Green. Relative expression of *TNF-α* (*B*) as well as *IL-12p40* and *NOS2* (*C*) was calculated with the Δ-ΔCt method as described in "Materials and Methods" using 18S rRNA as an internal control. Relative expression was calculated with respect to untreated controls.

protein assays that demonstrated synergism (Figs. 1 and 2). Indeed, quantitative real-time PCR analyses at peak times of transcript induction indicated that combined treatment resulted in enhanced transcript levels that were greater than additive relative to single treatments in both RAW 264.7 cells (Fig. 3*B*) and primary BMMs (Fig. 3*C*). Thus, the enhanced response to combined stimulation occurs in genes independent of direct ISRE control.

Although the synergy response occurs independent of ISRE control elements, this does not rule out the influence of possible secondary effects of IFN, such as up-regulation of TLRs or TLR signaling components that could regulate the enhanced response. To assess for secondary type I IFN affects, BMMs were treated in the absence or presence of neutralizing antibodies for IFN-α or IFN-β (Fig. 4), which were titered based on the ability to block the protective effects of the respective type I IFNs from EMCV challenge of L929 cells (data not shown). Whereas the IFN-α neutralizing antibody had no effect on NO production for any of the conditions of stimulation, the IFN-β neutralizing antibody inhibited the NO response to pIC alone (61% inhibition; $P = 0.003$), as well as the NO synergy response (63% inhibition; $P = 0.004$; Fig. 4*A*). The low-level NO response to CpG-ODN alone was also inhibited by neutralizing antibody for IFN-β ($P = 0.01$). In contrast, neutralizing IFN-α and IFN-β significantly enhanced the IL-12 response to combined stimulation (from 1.3- to 1.5-fold; Fig. 4*B*; $P < 0.03$). Interestingly, neither neutralizing antibody affected synergism for TNF-α (Fig. 4*C*) or IL-6 (Fig. 4*D*).

Because synergistic production of type I IFN with combined stimulation might explain why the neutralizing antibodies were ineffective for blocking cytokine production, induction of *IFN-β* was measured using RT-PCR of the cDNA samples obtained from RAW 264.7 cells treated in Fig. 3*A* to determine whether the IFN-β response itself was synergistic (Fig. 5*A*). Induction of *IFN-β* was detected with both pIC stimulation and combined stimulation but was only marginally detectable after CpG-ODN treatment (Fig. 5*A*). Interestingly, the level of *IFN-β* under conditions of combined stimulation did not appear greater than that observed with pIC alone. To obtain a more quantitative assessment of type I IFN production, *IFN-β* transcript levels were assessed 6 h after stimulation of BMMs by quantitative real-time PCR (Fig. 5*A*, *right panel*), and, indeed, *IFN-β* transcript levels were similar with pIC alone and the pIC + CpG combination. Viral protection assays that measure the effects of both IFN-α and IFN-β (Fig. 5*B*) were performed on culture supernatants from RAW 264.7 cells stimulated for 20 h with pIC and CpG, alone or in combination

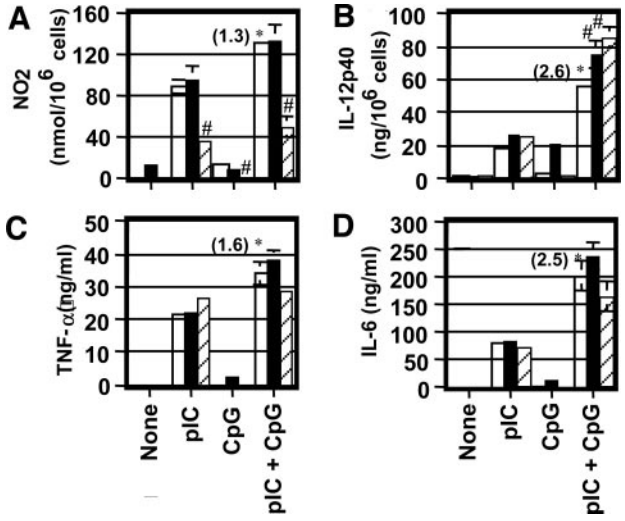

Fig. 4. Differential effects of type I IFN-neutralizing antibodies on (*A*) NO and (*B*−*D*) cytokine production in primary BMMs stimulated with pIC and CpG DNA. BMMs were stimulated with the indicated combinations of pIC and CpG-ODN for the indicated time in the presence of no antibody (□) or anti-IFN-α (■)-neutralizing or anti-IFN-β (▨)-neutralizing antibodies. Culture supernatants were assessed for (*A*) NO and (*B*) IL-12p40 24 h after stimulation or for (*C*) IL-6 or (*D*) TNF-α 6 h after stimulation as described above. *Bars* represent mean ± SE ($n = 3$) for a representative experiment that was reproduced at least twice. *Numbers in parentheses* represent the fold synergy for the combined treatment relative to the sum of the levels observed for each component treated alone. *Stars* represent significant ($P \leq 0.03$) interaction as determined by two-way ANOVA. *Pound symbol* (#) represents significant difference ($P \leq 0.01$) *versus* the same treatment in the absence of neutralizing antibody as assessed by a two-tailed Student's *t* test. Both neutralizing antibodies specifically blocked the protective effects of the appropriate type I IFN on L929 cells challenged with a lethal multiplicity of infection of EMCV.

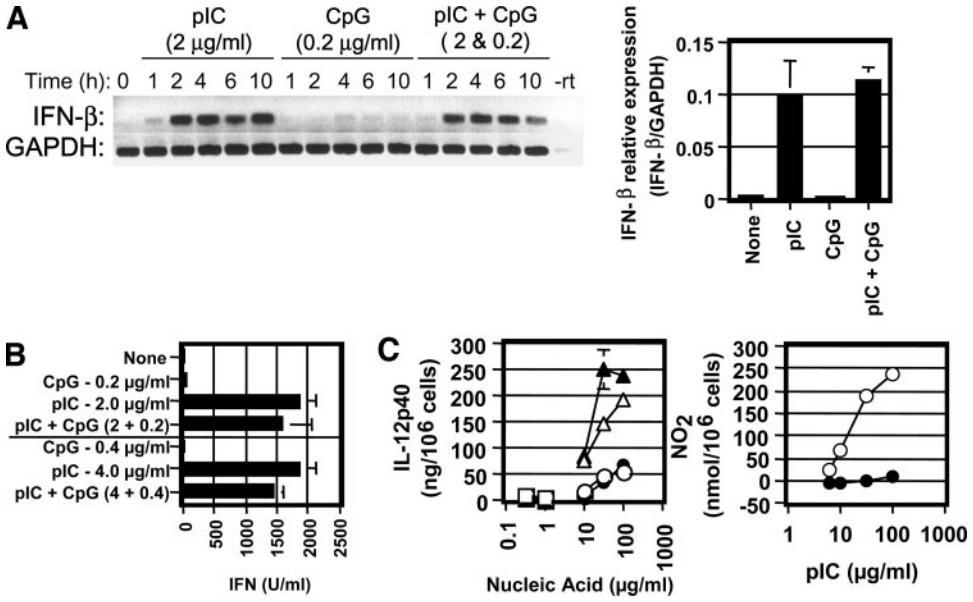

Fig. 5. Type I IFN production (*A* and *B*) and the role of the type I IFN-α/β receptor (*C*) in regulating synergism in murine macrophages. *A*, kinetics of IFN-β induction in RAW 264.7 cells. Reverse transcription-PCR analysis for *IFN-β* induction was performed using RAW cDNA samples from Fig. 3. Displayed is a negative image of a 2% agarose gel stained with ethidium bromide (*left panel*). Quantitative real-time PCR analysis of *IFN-β* transcript induction in primary BMMs stimulated for 6 h with pIC (10 μg/ml) and CpG-ODN (1 μg/ml), either alone or in combination (*right panel*), was performed. cDNA samples were obtained by reverse transcription, and copy number for murine *IFN-β* and *GAPDH* was obtained in comparison with corresponding standard curves using Molecular Beacon Probes specific for *IFN-β* and *GAPDH*. Normalized expression represents *IFN-β* copy number/*GAPDH* copy number. *B*, type I IFN (α and β) production in RAW 264.7 cells stimulated with pIC and CpG-ODN, either alone or in combination, at the indicated concentrations. RAW culture supernatants collected 20 h after stimulation were assessed for type I IFN by viral protection assays of L929 cells challenged with EMCV ("Materials and Methods"). *C*, synergism for IL-12p40 production in BMMs is independent of type I IFN-α/β receptor. Primary BMMs derived from wild-type (129SV, *open symbols*) and type I IFN-α/βR-KO (*filled symbols*) mice were stimulated with a varied concentration of pIC alone (*circles*), a varied concentration of CpG-ODN alone (*squares*), or a varied concentration of pIC plus 1 μg/ml CpG-ODN (*triangles*) for 24 h. Culture supernatants were measured for IL-12p40 by ELISA (*left panel*) or for nitrite by Griess assay (*right panel*). The lack of NO response to pIC stimulation (*right panel*) serves as a control indicating integrity of IFN-α/β receptor-KO. Each data point represents the mean ± SE for triplicate measure.

(Fig. 5*B*). Consistent with the IFN-β RT-PCR, there was no difference in type I IFN levels between treatments with pIC alone or pIC and CpG in combination. Thus, pIC and CpG do not display synergism for type I IFN production in murine macrophages. To confirm the results obtained with the neutralizing antibodies, primary BMMs derived from type I IFN receptor (IFNR)-knockout (KO) mice were stimulated with various concentrations of pIC and CpG-ODN, either alone or in combination (Fig. 5*C*, *left panel*). Indeed, synergism between pIC and CpG for eliciting IL-12p40 was maintained in IFNR-KO BMMs. The lack of NO response to pIC in IFNR-KO BMMs (Fig. 5*C*, *right panel*) indicates the integrity of IFNR gene deletion. Taken together, the studies on type I IFNs suggest that whereas IFN-β is an important component stimulating the synergism observed with NOS2, type I IFNs are not involved in regulating the enhanced proinflammatory cytokine response to combined stimulation with pIC and CpG-ODN.

Cotransfection of Human TLR3 and TLR9 Provides Enhanced Activation of the IL-8 Promoter after pIC Stimulation. A possible explanation for IFN-independent synergy is cooperativity between TLRs or their downstream signaling pathways. To assess the hypothesis that TLRs could combine for enhanced immunostimulation, human TLRs 1–9 were cotransfected with TLR3 into 293T cells, and activation of a luciferase reporter gene for the *IL-8* promoter was measured after stimulation with pIC (Fig. 6*A*). With the exception of TLR4, TLRs 1–8 provided a slight enhancement (1.5- to 2-fold) of the pIC-stimulated *IL-8* activation compared with transfections with TLR3 alone. The most potent combination of TLRs for pIC-stimulated *IL-8* activation, however, was TLR3 and TLR9 (Fig. 6*A*), *i.e.*, the TLRs for dsRNA and CpG DNA. This combination provided a nearly 4-fold enhancement of the response that was concentration-dependent (Fig. 6*B*). Although the mechanisms remain to be determined, it is clear that human TLR3 and TLR9 pathways specifically combine to provide an enhanced stimulatory effect.

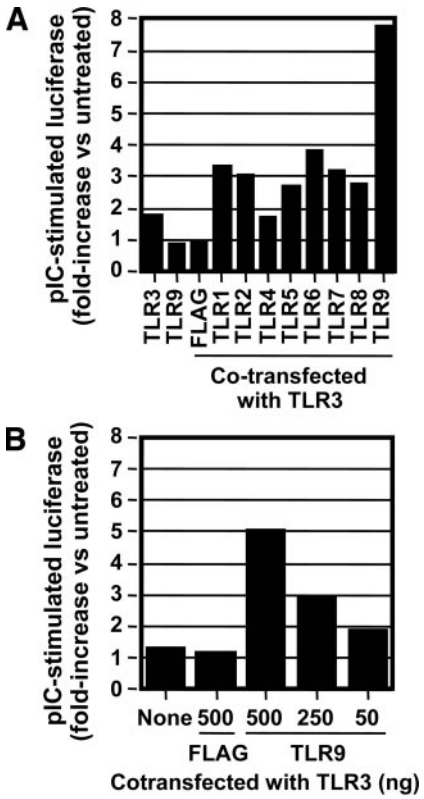

Fig. 6. Synergy between human TLR3 and TLR9 in activation of the IL-8 promotor by pIC. *A*, 293T cells were cotransfected with pRL-TK, pIL-8 promoter luciferase, and pTLR3 in the presence or absence of the indicated pTLR constructs. Transfected cells were stimulated with pIC (50 μg/ml) 36 h after transfection and assessed 16 h later for luciferase. *B*, 293T cells were cotransfected with pRL-TK, pIL-8 promoter luciferase, and pTLR3 in the presence of varied quantities of pTLR9 and assessed for pIC-stimulated luciferase as described in *A*.

Synergism for Proinflammatory Cytokine Production and Antitumor Activity *in Vivo*. We next wanted to assess whether synergism between dsRNA and CpG DNA occurred *in vivo*. To measure *in vivo* cytokine induction, serum was collected from C57BL/6 mice 4 h (*i.e.*, the peak time for IL-12 and IL-6 production) after intraperitoneal injection with PBS, pIC, CpG-ODN 1826, or the combination at the respective doses (Fig. 7, *A* and *B*). When doses of pIC and CpG-ODN were at or near the ED_{50} for eliciting IL-12p40, as determined in initial dose-response experiments with single agents (data not shown), the IL-12 response demonstrated significant ($P < 0.00005$) synergism that was 1.8-fold greater than additive levels (Fig. 7*A*). Whereas CpG-ODN alone did not stimulate detectable levels of IL-6, the same dose of CpG in combination with pIC stimulated levels of IL-6 (Fig. 7*B*) that were 2.3-fold greater than the response to pIC alone ($P < 0.00003$). Thus, similar to our observations using cultured macrophages, the systemic cytokine response to combined stimulation with pIC and CpG *in vivo* displayed synergism.

Because combined treatment elicited an enhanced innate response, we wanted to determine whether the combination could lead to an effective tumor immunotherapy. Mice were inoculated with 1×10^5 $B16\text{-}F_{10}$ melanoma cells, a murine melanoma model that is syngeneic in C57BL/6 mice, by tail vein injection. On day 3 after inoculation, mice were treated with either PBS, pIC, CpG-ODN 1826, or the combination by intraperitoneal injection at doses that elicited the synergistic cytokine response (Fig. 7, *A* and *B*). On day 17, mice were sacrificed, and lungs were excised, scored for lung tumor burden (Fig. 7*C*), and weighed to determine tumor mass (Fig. 7*D*). Combined treatment significantly ($P < 0.01$) reduced tumor burden by 37–40% compared with treatments with CpG-ODN or pIC alone, which had no significant effect on tumor burden relative to PBS-treated controls (Fig. 7*C*). Tumor mass was not significantly reduced by pIC treatment (Fig. 7*D*). In contrast, treatments with CpG alone and pIC and CpG in combination significantly ($P < 0.02$) reduced lung tumor mass compared with pIC treatment by 58% and 78%, respectively (Fig. 7*D*). Moreover, further reduction of tumor mass by combined treatment approached significance ($P = 0.05$) in comparison with mice treated with CpG alone. Thus, using both measures, combined treatment had an enhanced antitumor response relative to treatments with single agents.

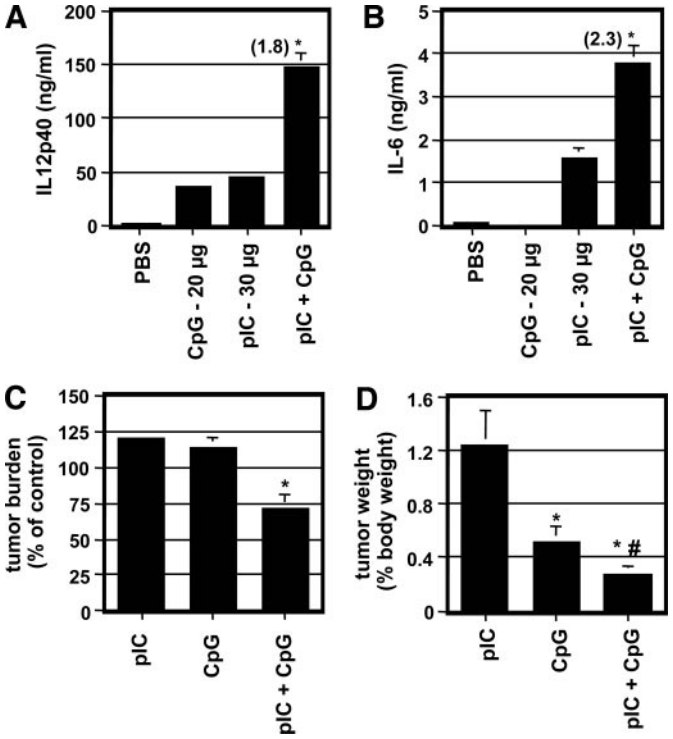

Fig. 7. *In vivo* coadministration of pIC and CpG-ODN in mice elicits a synergistic proinflammatory cytokine response (*A* and *B*) that correlates with an enhanced antitumor effect against established $B16\text{-}F_{10}$ pulmonary metastases (*C* and *D*). *A* and *B*, C57BL/6 mice were treated with pIC and CpG-ODN, either alone or in combination, at the indicated doses (μg/mouse) by intraperitoneal injection. Four hours after treatment, serum was collected and assessed for IL-12p40 (*A*) or IL-6 (*B*) by ELISA. *Bars* represent the mean ± SE ($n = 6$ mice) pooled from two independent experiments. *Stars* represent significant ($P < 0.00005$) interaction as determined by two-way ANOVA. *C* and *D*, combined treatment of C57BL/6 mice bearing established $B16\text{-}F_{10}$ pulmonary metastases with pIC and CpG-ODN significantly reduces lung tumor burden (*C*) and lung tumor mass (*D*) relative to treatments with single agents. C57BL/6 mice received injection of 1×10^5 $B16\text{-}F_{10}$ cells by tail vein injection. Using a dose combination that displayed synergism for eliciting IL-12 and IL-6, mice were treated with PBS (*i.e.*, control mice) or pIC (30 μg/mouse) and CpG-ODN (20 μg/mouse) alone and in combination 3 days after tumor inoculation. On day 17, lungs were excised from mice and weighed, and tumors were counted under a dissecting microscope. *C*, tumor burden was normalized to PBS-treated controls as described in "Materials and Methods." *D*, tumor mass was calculated as the percentage of body weight of tumor-bearing lungs minus the average percentage of body weight of tumor-free lungs (1.2% body weight) as described in "Materials and Methods." *Bars* represent mean ± SE ($n = 5–6$) for a representative experiment that was reproduced twice. Tumor burden and tumor mass for pIC-treated mice were not significantly different from those of PBS-treated controls.

Because macrophages demonstrated synergism for NO production *in vitro* and NO released from activated macrophage can possess tumoricidal activity, the lungs of tumor-bearing mice were assessed for NOS2 expression. Mice were inoculated with $B16\text{-}F_{10}$ tumor cells and treated with PBS, pIC (30 μg/mouse), CpG-ODN (20 μg/mouse), or pIC + CpG-ODN as described in the above-mentioned experiments. Twenty-four hours after treatment, whole cell extracts from lungs were collected and assessed for NOS2 expression (Fig. 8*A*) by Western blot analysis. Treatment with pIC did not enhance NOS2 expression in lungs relative to PBS-treated mice, whereas treatment with CpG-ODN increased NOS2 expression (Fig. 8*A*). The pIC and CpG combination resulted in a further enhancement of NOS2 expression relative to treatment with CpG alone (note that β-actin loading controls indicate protein overloading in CpG lanes relative to other treatments). All treatments increased NK cell activation relative to PBS treatment at 24 h, as indicated by flow cytometric analysis showing increased CD69 expression on NK1.1+ cells in splenocytes harvested at the same time as lungs; however, NK activation was not further enhanced by combined treatment relative to treatments with pIC or CpG-ODN alone (data not shown). Thus, whereas both innate immune effector mechanisms with tumoricidal activity were stimulated, only macrophage NOS2 showed further enhancement by combined treatment relative to treatments with pIC or CpG-ODN alone.

The $B16\text{-}F_{10}$ model of experimental pulmonary metastasis is poorly immunogenic as a result of down-regulated MHC expression and antigen processing similar to some human tumors (42, 43). However, immunization of mice with tumor-associated antigens (TAAs) using pSIN, as well as other vaccination strategies, is capable of breaking immunological tolerance to $B16\text{-}F_{10}$, resulting in acquired responses to melanoma TAAs (5, 44). Thus, in addition to innate effector responses such as macrophage NO production and NK activity that are capable of direct tumoricidal activities, antigen presentation mediated by DCs may also be an important innate mechanism that facilitates development of acquired antitumor responses. To measure DC maturation, splenocyte preparations were collected from the mice described in Fig. 8*A* at 24 h, and expression of DC antigen presentation markers was analyzed by flow cytometry (Fig. 8*B*). As expected, class I MHC expression (Fig. 8*B*, *left column*) was positive on all cells gated for the DC marker CD11c (Fig. 8*B*). All treatments stimulated increased class I expression, as indicated by the shift in mean fluorescence intensity (MFI), relative to PBS-treated controls (*gray-shaded histograms*), with the greatest shift occurring in the combined treatment group (MFIs for entire class I histograms are not shown but were 76 for PBS, 155 for pIC, 165 for CpG, and 195 for pIC + CPG;

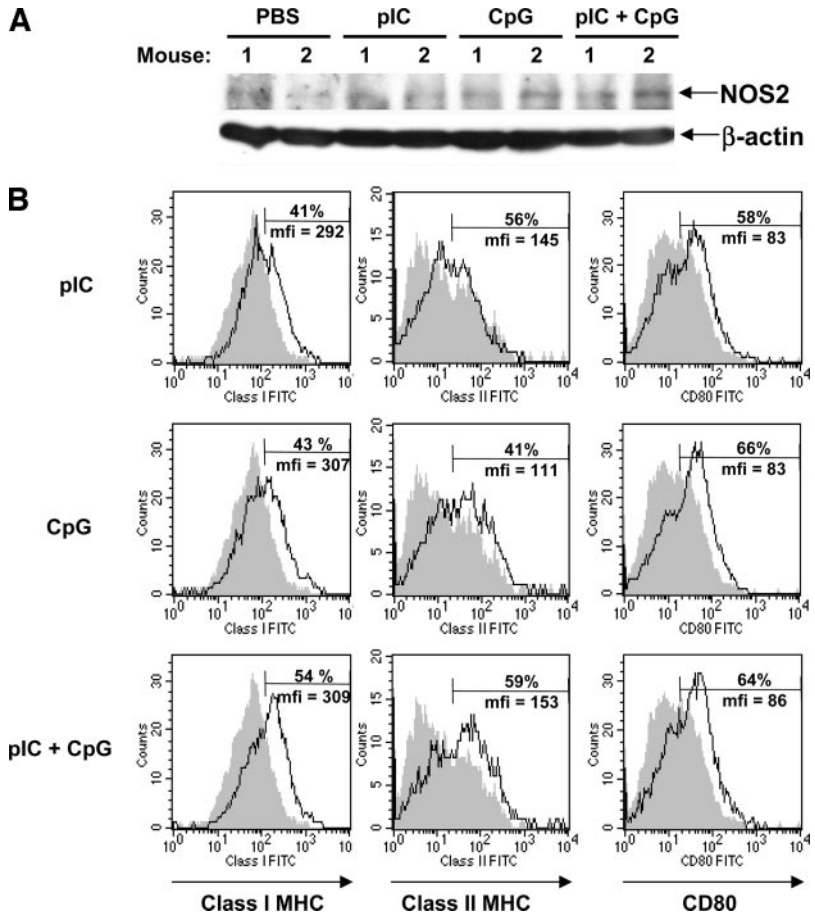

Fig. 8. Treatment of mice with pIC and CpG-ODN in combination stimulates enhanced NOS2 expression in the lung (*A*) and promotes splenic DC antigen presentation (*B*). Three days after tumor inoculation, C57BL/6 mice were treated with pIC (30 μg/mouse) and CpG-ODN (20 μg/mouse), either alone or in combination, by intraperitoneal injection. Twenty-four hours after treatment, lungs (*A*) and spleens (*B*) were excised for analysis. *A*, whole cell extracts from lung tissue (80 μg protein/lane) were analyzed for expression of NOS2 and β-actin (as a loading control) by Western blot. *B*, splenocytes pooled from 2 mice/group were analyzed for coexpression of the DC marker CD11c and the indicated marker for antigen presentation (class I MHC, class II MHC, or CD80) by two-color flow cytometry. A histogram is displayed for expression of class I MHC (*left column*), class II MHC (*middle column*), or CD80 (*right column*) in cells gated for CD11c expression (5–10% of total splenocytes, where isotype control antibody for CD11c stained <1%). The *shaded histogram* represents expression of the indicated antigen presentation marker in CD11c-positive splenocytes from PBS-treated controls. The *black line histograms* represent expression measured in CD11c-positive splenocytes of mice treated as indicated. The delineated region for class I MHC (*left column*) encompasses a peak for high class I expression. The regions delineated for class II MHC (*middle column*) and CD80 (*right column*) indicate positive expression of class II MHC or CD80 where istoype control antibodies stained <1% of cells in this region, which did not vary with treatment. The percentages represent the percentage of CD11c-positive cells from treated mice within the indicated region, and MFI indicates the MFI for that population of cells. For PBS-treated mice, 16% of CD11c-positive cells were in the high class I MHC region (MFI = 215), 33% of CD11c-positive cells were positive for class II MHC (MFI = 143), and 38% of CD11c-positive cells were positive for CD80 expression (MFI = 79). Data are representative of two independent experiments that provided essentially identical results.

Fig. 8*B*). In PBS-treated controls, 16% of CD11c-positive cells had high class I MHC levels, as indicated by the delineated region. All treatments increased the percentage of cells within this region, with the combined treatment showing the greatest percentage increase (pIC = 41%, CpG = 43%, and pIC + CpG = 54%). Thus, whereas all treatments increased class I expression, combined treatment with pIC and CpG demonstrated the greatest enhancement. In PBS-treated mice, 33% of CD11c-positive cells were positive for class II MHC (Fig. 8*B*, *middle column*; MFI in the delineated region of the shaded plot = 143). Treatments with pIC and CpG alone increased the percentage of DCs positive for class II to 56% and 41%, respectively, with no change or a reduction in MFI (MFI for pIC = 144; MFI for CpG = 111). Combined treatment increased class II expression in terms of both percentage (59%) and MFI (MFI = 153). Thus, combined treatment with pIC and CpG DNA resulted in the greatest enhancement of class II expression on DCs (similar to expression of class I, but to a lesser degree). Analysis of the costimulatory molecule CD80 (Fig. 8*B*, *right column*) revealed that all treatments increased CD80 expression (as indicated in the delineated region) on DCs relative to PBS (PBS = 38% with MFI of 79, pIC = 58% with MFI of 83, CpG = 66% with MFI of 83, and pIC + CpG = 64% with MFI of 86). Thus, all treatments enhanced the costimulatory function of DCs indicating maturation; however, combined treatment did not elicit further enhancement. Taken together, these data suggest that treatment with pIC and CpG-ODN in combination stimulated DC maturation with an increased capacity to present antigen through class I and class II MHC relative to treatments with either agent alone. Moreover, the obligatory costimulatory factors for antigen presentation were activated.

DISCUSSION

These studies provide the first description and characterization of synergism between dsRNA and CpG DNA response pathways. Synergism was observed for the induction of NOS2, IL-12p40, TNF-α, and IL-6 in murine macrophages, all of which play important roles in innate immunity during a developing immune response. Although dsRNA and CpG DNA did not cause synergistic induction of IFN-β, IFN neutralization studies demonstrate that paracrine or autocrine effects of IFN-β are important for NOS2 synergy. Interestingly, mechanisms of synergy independent of IFN-β contribute to the IL-12p40, TNF-α, and IL-6 responses. In support of the studies with IFN-neutralizing antibodies, synergism for IL-12p40 production was maintained in BMMs from type I IFNR-KO mice. This is not surprising because these cytokines are generally not responsive to IFN and lack ISREs in their promoters. In support of IFN-independent mechanisms regulating synergy, cotransfection of human TLR3 and TLR9 caused a synergistic activation of the *IL-8* reporter construct in response to dsRNA stimulation (Fig. 5), suggesting that components of TLR3 and TLR9 signaling pathways can combine in a synergistic manner. Moreover, the data also show that synergism between these pathways can occur in human cells. With *in vivo* studies, combined treatment of mice with pIC and CpG stimulated greater than additive levels of cytokine that correlated with enhanced inhibition of the growth of established B16-F_{10} pulmonary metastases in comparison with treatments using the single agents alone. Furthermore, combined treatment resulted in enhanced expression of NOS2 in the lungs of tumor-bearing mice. Finally, combined treatment resulted in enhanced class I MHC levels in splenic DCs that were capable of the antigen

presentation function, suggesting a mechanism of antigen cross-presentation may be facilitated by combined treatment.

We hypothesize that the combined effects of dsRNA and CpG DNA mimic infections with large DNA viruses; thus, the heightened response is indicative of a two-signal biological response, a recurrent theme throughout the immune system, to the presence of two PAMPs from an invading pathogen. Double-stranded RNA is a viral replication intermediate that has long been recognized as a PAMP associated with viral infection, including infections with large DNA viruses. Indeed, several large DNA viruses have acquired strategies of immune avoidance that circumvent the host intracellular dsRNA response pathways (45–47). Although CpG DNA is generally referred to as a "bacterial" product, recent evidence confirms that CpG DNA is a viral PAMP. The CpG dinucleotide occurs at a similar frequency in most invertebrates (16), and large DNA viruses (>30 kb) such as cytomegalovirus have a similar CpG DNA frequency as *Escherichia coli* (17). Isolates of DNA from viruses with similar relative abundance of CpG to bacterial DNA have immunostimulatory properties (18, 19). Finally, TLR9 is required for pDC recognition of HSV and concomitant IFN-α production (20, 21). Thus, it is clear that dsRNA and CpG DNA represent PAMPs that are present during infections with large DNA viruses. Another circumstance in which synergy between these PAMPs may be advantageous to the host is in the case of superinfection, such as an RNA respiratory viral infection leaving the host susceptible to bacterial infection. Thus, the combined recognition of dsRNA and CpG DNA could represent definitive recognition of virus or identification of severe infection, with either case warranting an amplified immune response. Moreover, our data suggest that an intriguing byproduct of this amplified response is enhanced antitumor activity.

It is of interest that treatments stimulating the greatest increase in lung NOS2 expression (Fig. 8*A*), *i.e.*, CpG-ODN alone and in combination with pIC, were most effective for inhibiting tumor growth (Fig. 7*D*). It remains to be determined whether the enhanced NOS2 expression is a result of direct synergism in activating macrophages or an enhancement of macrophage infiltration into the lung. In either case, heightened NO release from macrophages near tumor foci in the lung could induce NO-dependent apoptosis in the tumors (48–50). Recent evidence suggests that cross presentation of TAAs by DCs is more effective when TAAs are provided in apoptotic bodies in comparison with antigens loaded as soluble extracts (44, 51). The B16-F_{10} melanoma lacks class I MHC expression (43, 52); thus, a mechanism such as DC cross-presentation is likely required to elicit acquired antitumor immune responses. Indeed, pSIN-based vaccines that contain both dsRNA and CpG DNA are capable of breaking immunological tolerance to B16-F_{10} TAAs (5, 8). Therefore, it is plausible that, in our system, whereas all treatments elicited NK activation to similar levels, an enhanced apoptotic response in established tumors resulting from macrophage NO production provided an optimal substrate for enhanced DC cross-presentation (*i.e.*, apoptotic B16-F_{10} melanoma cells). Therefore, it is of high interest to determine whether the pIC and CpG-ODN combination can (*a*) induce heightened NO-dependent apoptotic responses at tumor sites and (*b*) stimulate improved acquired antitumor immune responses relative to treatment with single agents. Thus, the improved antitumor effect may arise from heightened innate effector responses in combination with the capacity of DCs to cross-present TAAs.

Synergism between dsRNA and CpG DNA for activating innate responses may also explain the improved efficacy of pSIN-based plasmid DNA vaccines for generating antigen-specific acquired responses in comparison with pCMV-based vaccines. Whereas additional studies with the pSIN system are needed to confirm this hypothesis, our observations suggest that dsRNA produced by the Sindbis replicon in pSIN, in combination with CpG DNA inherent in the plasmid, is likely to enhance IL-12 production. IL-12 represents an important cytokine that stimulates NK cytotoxicity and induces the production of IFN-γ from NK cells and T cells, which can feedback on antigen-presenting cells promoting antigen presentation (53–57). Thus, enhanced IL-12 production resulting from dsRNA and CpG DNA in pSIN could bridge innate immunity with acquired responses (30), thereby accounting for the efficacy of pSIN. Thus, these studies justify further exploration of the combined use of pIC and CpG-ODN as adjuvants during vaccination.

Our data as well as published reports suggest that regulation of the synergy response at the cellular level is complex, involving both primary and secondary components. It is known that promoter elements that respond to TLR signaling, *i.e.*, NF-κB and AP-1, can cooperate in regulating transcription (58–61). Moreover, these TLR-regulatory elements can cooperate with ISREs, which are controlled by type I IFN receptor signaling, to positively regulate *NOS2*, thereby facilitating synergy at the transcriptional level (35, 39, 62). In our system, it is likely that pIC, through TLR3 and perhaps other dsRNA PRRs, stimulates IFN-β production that can feedback in an autocrine/paracrine manner, resulting in cooperative induction of NOS2 through interactions of TLR elements and ISREs in the *NOS2* promoter (35, 39). In apparent contradiction to this, however, the *IFN-β* response itself does not demonstrate synergy, even though its promoter possesses NF-κB, AP-1, and consensus IFN response sites (63, 64). *IFN-β* induction through dsRNA stimulation of TLR3 and PKR is mediated by IFN-regulatory factor (IRF)-3 (41, 65, 66). In the context of the *IFN-β* promoter, IRF-3 is the primary regulator of transcriptional activation that can override relatively weak activation that occurs at NF-κB and AP-1 sites (41). An indication that the system is even more complex is the apparent antagonism of IL-12p40 by type I IFN (Figs. 4*B* and 5*C*). These observations are in agreement with recent studies of type I IFN antagonism of IL-12 production (67). In addition, *IL-12p40* induction has been reported to be controlled through TLR elements as well as the IRF family member IFN consensus sequence-binding protein (or IRF-8; Refs. 68). Thus, constitutive or induced expression of IRF family members may be involved in regulating the enhanced response observed here.

Evidence of a direct interaction between the dsRNA and TLR9 signaling pathways is provided by our data. First, it is clearly established that synergism for cytokine production occurred independent of the autocrine/paracrine effects of type I IFN. Indeed, the observation that IL-12p40 synergism was maintained in BMMs from type I IFNR-KO mice (Fig. 5*C*) confirmed results in which neutralizing antibodies for type I IFN did not affect cytokine production (Fig. 4). Second, whereas dsRNA by itself is sufficient to activate TLR elements and ISREs, the contribution of CpG DNA is required for maximal, synergistic NO response. Because the enhanced response is not accounted for by greater IFN production (Fig. 5, *A* and *B*), the combined effects of dsRNA and CpG DNA likely result from complementary or cooperative recruitment of components of the dsRNA and TLR9 signaling pathways. Finally, the enhanced activation of the IL-8 promoter in TLR3 and TLR9 cotransfection experiments (Fig. 6) supports the notion that the TLR3 and TLR9 pathways cooperate with each other for activation. What remains to be determined is the mechanism of interaction. Indeed, it will be of interest to determine whether synergism occurs through mechanisms such as TLR3/TLR9 heterodimerization, corecruitment of the TLR adapter molecules TRIF for TLR3 (65, 66) and MyD88 for TLR9 (69, 70), or interaction of signaling components more distal to receptor ligation such as complementary activation of transcription factors (71).

The role of IFN-β in mediating the NOS2 synergy response to dsRNA and CpG DNA is consistent with other reports of synergy

between the IFN system and TLR signaling pathways. Indeed, Toshchakov *et al.* (35) have demonstrated that IFN-β mediates NOS2 induction after stimulation with TLR4 agonists in mouse macrophages. Moreover, pretreatment with type I or type II IFNs can potentiate NOS2 induction by LPS and CpG DNA, respectively (39, 72). Indeed, pretreatment with LPS, a strong IFN inducer in macrophages, can act in synergy with CpG DNA for NOS2 induction (73). In support of this, cDNA microarray analyses by our group[4] show that components of the TLR signaling pathways (MyD88, TIRAP, TLR9, and TLR3) are induced after IFN stimulation. The interaction between dsRNA and CpG DNA reported here appears similar in that a strong IFN inducer (dsRNA) and CpG DNA resulted in an enhanced NOS2 response. Our system differs, however, because the agents are simultaneously added to the culture medium or injected into mice. In treatment of cultured cells, c-Jun-NH_2-terminal kinase and p38 mitogen-activated protein kinase phosphorylation can be observed within 10 min after stimulation with pIC alone, CpG alone, and the combination (data not shown), suggesting that the dsRNA and CpG DNA pathways are present and gene induction is not required to initiate the response. Taken together, the regulation of dsRNA and CpG DNA synergism is likely to arise from both primary and secondary responses resulting in a complex interaction of TLR, type I IFNR, IRF, and likely other signaling pathways.

These studies represent the first characterization of an interaction between dsRNA and CpG DNA response pathways resulting in heightened innate immune activation. Whereas the immune mechanisms that coordinate to provide the enhanced antitumor response remain to be elucidated, it is clear that both ligands activate a number of immune functions that are capable of inhibiting tumor growth including type I IFN production, NK activation, macrophage NO production, and proinflammatory cytokine production. Regulation of the synergy response is complex, involving multiple signaling pathways from both primary (dsRNA and CpG DNA) and secondary (IFN-β and perhaps others) stimuli. Indeed, synergism between dsRNA and CpG pathways is important not only for understanding innate responses to viral and bacterial infection but also in the context of cancer vaccination and tumor immunotherapy. Thus, additional studies exploring this interaction will lead to an improved understanding of (*a*) the innate responses to pathogen infection and (*b*) the utility for pIC and CpG-ODN in immune-based therapies for cancer.

REFERENCES

1. Ahmad-Nejad P, Hacker H, Rutz M, et al. Bacterial CpG-DNA and lipopolysaccharides activate Toll-like receptors at distinct cellular compartments. Eur J Immunol 2002;32:1958–68.
2. Stark GR, Kerr IM, Williams BR, Silverman RH, Schreiber RD. How cells respond to interferons. Annu Rev Biochem 1998;67:227–64.
3. Aderem A, Ulevitch RJ. Toll-like receptors in the induction of the innate immune response. Nature (Lond) 2000;406:782–7.
4. MacMicking J, Xie Q-W, Nathan CF. Nitric oxide and macrophage function. Annu Rev Immunol 1997;15:323–50.
5. Leitner WW, Hwang LN, De Veer MJ, et al. Alphavirus-based DNA vaccine breaks immunological tolerance by activating innate antiviral pathways. Nat Med 2003;9:33–9.
6. Whitmore MM, Li S, Falo L Jr, Huang L. Systemic administration of LPD prepared with CpG oligonucleotides inhibits the growth of established pulmonary metastases by stimulating innate and acquired antitumor immune responses. Cancer Immunol Immunother 2001;50:503–14.
7. Lanuti M, Rudginsky S, Force SD, et al. Cationic lipid:bacterial DNA complexes elicit adaptive cellular immunity in murine intraperitoneal tumor models. Cancer Res 2000;60:2955–63.
8. Leitner WW, Ying H, Driver DA, Dubensky TW, Restifo NP. Enhancement of tumor-specific immune response with plasmid DNA replicon vectors. Cancer Res 2000;60:51–5.
9. Ying H, Zaks TZ, Wang RF, et al. Cancer therapy using a self-replicating RNA vaccine. Nat Med 1999;5:823–7.
10. Scheule RK. The role of CpG motifs in immunostimulation and gene therapy. Adv Drug Deliv Rev 2000;44:119–34.
11. McCluskie MJ, Weeratna RD, Davis HL. The role of CpG in DNA vaccines. Springer Semin Immunopathol 2000;22:125–32.
12. Paludan SR, Mogensen SC. Virus-cell interactions regulating induction of tumor necrosis factor alpha production in macrophages infected with herpes simplex virus. J Virol 2001;75:10170–8.
13. Smith EJ, Marie I, Prakash A, Garcia-Sastre A, Levy DE. IRF3 and IRF7 phosphorylation in virus-infected cells does not require double-stranded RNA-dependent protein kinase R or Ikappa B kinase but is blocked by vaccinia virus E3L protein. J Biol Chem 2001;276:8951–7.
14. Clarke PA, Mathews MB. Interactions between the double-stranded RNA binding motif and RNA: definition of the binding site for the interferon-induced protein kinase DAI (PKR) on adenovirus VA RNA. RNA 1995;1:7–20.
15. Desai SY, Patel RC, Sen GC, et al. Activation of interferon-inducible 2′-5′ oligoadenylate synthetase by adenoviral VAI RNA. J Biol Chem 1995;270:3454–61.
16. Burge C, Campbell AM, Karlin S. Over- and under-representation of short oligonucleotides in DNA sequences. Proc Natl Acad Sci USA 1992;89:1358–62.
17. Karlin S, Doerfler W, Cardon LR. Why is CpG suppressed in the genomes of virtually all small eukaryotic viruses but not in those of large eukaryotic viruses? J Virol 1994;68:2889–97.
18. Krieg AM, Wu T, Weeratna R, et al. Sequence motifs in adenoviral DNA block immune activation by stimulatory CpG motifs. Proc Natl Acad Sci USA 1998;95:12631–6.
19. Zheng M, Klinman DM, Gierynska M, Rouse BT. DNA containing CpG motifs induces angiogenesis. Proc Natl Acad Sci USA 2002;99:8944–9.
20. Krug A, Luker GD, Barchet W, et al. Herpes simplex virus type 1 (HSV-1) activates murine natural interferon-producing cells (IPC) through Toll-like receptor 9. Blood 2004;103:1433–7.
21. Lund J, Sato A, Akira S, Medzhitov R, Iwasaki A. Toll-like receptor 9-mediated recognition of herpes simplex virus-2 by plasmacytoid dendritic cells. J Exp Med 2003;198:513–20.
22. Alexopoulou L, Holt AC, Medzhitov R, Flavell RA. Recognition of double-stranded RNA and activation of NF-kappaB by Toll-like receptor 3. Nature (Lond) 2001;413:732–8.
23. Kumar A, Yang YL, Flati V, et al. Deficient cytokine signaling in mouse embryo fibroblasts with a targeted deletion in the PKR gene: role of IRF-1 and NF-kappaB. EMBO J 1997;16:406–16.
24. Khabar KS, Dhalla M, Siddiqui Y, et al. Effect of deficiency of the double-stranded RNA-dependent protein kinase, PKR, on antiviral resistance in the presence or absence of ribonuclease L: HSV-1 replication is particularly sensitive to deficiency of the major IFN-mediated enzymes. J Interferon Cytokine Res 2000;20:653–9.
25. Zhou A, Paranjape J, Brown TL, et al. Interferon action and apoptosis are defective in mice devoid of 2′,5′-oligoadenylate-dependent RNase L. EMBO J 1997;16:6355–63.
26. Hemmi H, Takeuchi O, Kawai T, et al. A Toll-like receptor recognizes bacterial DNA. Nature (Lond) 2000;408:740–5.
27. Bauer S, Kirschning CJ, Hacker H, et al. Human TLR9 confers responsiveness to bacterial DNA via species-specific CpG motif recognition. Proc Natl Acad Sci USA 2001;98:9237–42.
28. Stuehr DJ, Nathan CF. Nitric oxide. A macrophage product responsible for cytostasis and respiratory inhibition in tumor target cells. J Exp Med 1989;169:1543–55.
29. Cella M, Sallusto F, Lanzavecchia A. Origin, maturation and antigen presenting function of dendritic cells. Curr Opin Immunol 1997;9:10–6.
30. Fearon DT, Locksley RM. The instructive role of innate immunity in the acquired immune response. Science (Wash DC) 1996;272:50–3.
31. Brittenden J, Heys SD, Ross J, Eremin O. Natural killer cells and cancer. Cancer (Phila) 1996;77:1226–43.
32. Herberman RB. Cancer immunotherapy with natural killer cells. Semin Oncol 2002;29:27–30.
33. Cowdery JS, Boerth NJ, Norian LA, Myung PS, Koretzky GA. Differential regulation of the IL-12 p40 promoter and of p40 secretion by CpG DNA and lipopolysaccharide. J Immunol 1999;162:6770–5.
34. Overbergh L, Valckx D, Waer M, Mathieu C. Quantification of murine cytokine mRNAs using real time quantitative reverse transcriptase PCR. Cytokine 1999;11:305–12.
35. Toshchakov V, Jones BW, Perera PY, et al. TLR4, but not TLR2, mediates IFN-beta-induced STAT1alpha/beta-dependent gene expression in macrophages. Nat Immunol 2002;3:392–8.
36. Cowdery JS, Chace JH, Yi AK, Krieg AM. Bacterial DNA induces NK cells to produce IFN-gamma in vivo and increases the toxicity of lipopolysaccharides. J Immunol 1996;156:4570–5.
37. Chou TC, Talalay P. Quantitative analysis of dose-effect relationships: the combined effects of multiple drugs or enzyme inhibitors. Adv Enzyme Regul 1984;22:27–55.
38. Slinker BK. The statistics of synergism. J Mol Cell Cardiol 1998;30:723–31.
39. Ohmori Y, Hamilton TA. Requirement for STAT1 in LPS-induced gene expression in macrophages. J Leukocyte Biol 2001;69:598–604.
40. Brehm G, Kirchner H. Analysis of the interferons induced in mice in vivo and in macrophages in vitro by Newcastle disease virus and by polyinosinic-polycytidylic acid. J Interferon Res 1986;6:21–8.
41. Peters KL, Smith HL, Stark GR, Sen GC. IRF-3-dependent, NFkappa B- and JNK-independent activation of the 561 and IFN-beta genes in response to double-stranded RNA. Proc Natl Acad Sci USA 2002;99:6322–7.
42. Li M, Muller J, Xu F, Hearing VJ, Gorelik E. Inhibition of melanoma-associated antigen expression and ecotropic retrovirus production in B16BL6 melanoma cells transfected with major histocompatibility complex class I genes. Cancer Res 1996;56:4464–74.
43. Chiang EY, Henson M, Stroynowski I. Correction of defects responsible for impaired Qa-2 class Ib MHC expression on melanoma cells protects mice from tumor growth. J Immunol 2003;170:4515–23.

44. Goldszmid RS, Idoyaga J, Bravo AI, et al. Dendritic cells charged with apoptotic tumor cells induce long-lived protective CD4+ and CD8+ T cell immunity against B16 melanoma. J Immunol 2003;171:5940–7.
45. Mellits KH, Kostura M, Mathews MB. Interaction of adenovirus VA RNAl with the protein kinase DAI: nonequivalence of binding and function. Cell 1990;61:843–52.
46. Khoo D, Perez C, Mohr I. Characterization of RNA determinants recognized by the arginine- and proline-rich region of Us11, a herpes simplex virus type 1-encoded double-stranded RNA binding protein that prevents PKR activation. J Virol 2002;76: 11971–81.
47. Xiang Y, Condit RC, Vijaysri S, et al. Blockade of interferon induction and action by the E3L double-stranded RNA binding proteins of vaccinia virus. J Virol 2002;76: 5251–9.
48. Huerta-Yepez S, Vega M, Jazirehi A, et al. Nitric oxide sensitizes prostate carcinoma cell lines to TRAIL-mediated apoptosis via inactivation of NF-kappaB and inhibition of Bcl-(xL) expression. Oncogene 2004;23:4993–5003.
49. Bhaumik S, Khar A. Cytokine-induced production of NO by macrophages induces apoptosis and immunological rejection of AK-5 histiocytic tumor. Apoptosis 1998; 3:361–8.
50. Chawla-Sarkar M, Bauer JA, Lupica JA, et al. Suppression of NF-kappa B survival signaling by nitrosylcobalamin sensitizes neoplasms to the anti-tumor effects of Apo2L/TRAIL. J Biol Chem 2003;278:39461–9.
51. Scheffer SR, Nave H, Korangy F, et al. Apoptotic, but not necrotic, tumor cell vaccines induce a potent immune response in vivo. Int J Cancer 2003;103:205–11.
52. Xu F, Carlos T, Li M, et al. Inhibition of VLA-4 and up-regulation of TIMP-1 expression in B16BL6 melanoma cells transfected with MHC class I genes. Clin Exp Metastasis 1998;16:358–70.
53. Lieberman LA, Hunter CA. Regulatory pathways involved in the infection-induced production of IFN-gamma by NK cells. Microbes Infect 2002;4:1531–8.
54. Trinchieri G. Interleukin-12 and the regulation of innate resistance and adaptive immunity. Nat Rev Immunol 2003;3:133–46.
55. Colombo MP, Trinchieri G. Interleukin-12 in anti-tumor immunity and immunotherapy. Cytokine Growth Factor Rev 2002;13:155–68.
56. Basse PH, Whiteside TL, Chambers W, Herberman RB. Therapeutic activity of NK cells against tumors. Int Rev Immunol 2001;20:439–501.
57. Banchereau J, Paczesny S, Blanco P, et al. Dendritic cells: controllers of the immune system and a new promise for immunotherapy. Ann N Y Acad Sci 2003;987:180–7.
58. Feng SH, Lo SC. Lipid extract of Mycoplasma penetrans proteinase K-digested lipid-associated membrane proteins rapidly activates NF-kappaB and activator protein 1. Infect Immun 1999;67:2951–6.
59. Udalova IA, Kwiatkowski D. Interaction of AP-1 with a cluster of NF-kappa B binding elements in the human TNF promoter region. Biochem Biophys Res Commun 2001;289:25–33.
60. Ma W, Gee K, Lim W, et al. Dexamethasone inhibits IL-12p40 production in lipopolysaccharide-stimulated human monocytic cells by down-regulating the activity of c-Jun N-terminal kinase, the activation protein-1, and NF-kappaB transcription factors. J Immunol 2004;172:318–30.
61. Naumann M, Wessler S, Bartsch C, Wieland B, Meyer TF. Neisseria gonorrhoeae epithelial cell interaction leads to the activation of the transcription factors nuclear factor kappaB and activator protein 1 and the induction of inflammatory cytokines. J Exp Med 1997;186:247–58.
62. Lowenstein CJ, Alley EW, Raval P, et al. Macrophage nitric oxide synthase gene: two upstream regions mediate induction by interferon gamma and lipopolysaccharide. Proc Natl Acad Sci USA 1993;90:9730–4.
63. Kirchhoff S, Wilhelm D, Angel P, Hauser H. NFkappaB activation is required for interferon regulatory factor-1- mediated interferon beta induction. Eur J Biochem 1999;261:546–54.
64. Ludwig S, Ehrhardt C, Neumeier ER, et al. Influenza virus-induced AP-1-dependent gene expression requires activation of the JNK signaling pathway. J Biol Chem 2001;276:10990–8.
65. Yamamoto M, Sato S, Mori K, et al. Cutting edge: a novel Toll/IL-1 receptor domain-containing adapter that preferentially activates the IFN-beta promoter in the Toll-like receptor signaling. J Immunol 2002;169:6668–72.
66. Yamamoto M, Sato S, Hemmi H, et al. Role of adaptor TRIF in the MyD88-independent toll-like receptor signaling pathway. Science (Wash DC) 2003;301: 640–3.
67. Byrnes AA, Ma X, Cuomo P, et al. Type I interferons and IL-12: convergence and cross-regulation among mediators of cellular immunity. Eur J Immunol 2001;31: 2026–34.
68. Scharton-Kersten T, Contursi C, Masumi A, Sher A, Ozato K. Interferon consensus sequence binding protein-deficient mice display impaired resistance to intracellular infection due to a primary defect in interleukin 12 p40 induction. J Exp Med 1997;186:1523–34.
69. Hacker H, Vabulas RM, Takeuchi O, et al. Immune cell activation by bacterial CpG-DNA through myeloid differentiation marker 88 and tumor necrosis factor receptor-associated factor (TRAF)6. J Exp Med 2000;192:595–600.
70. Schnare M, Holt AC, Takeda K, Akira S, Medzhitov R. Recognition of CpG DNA is mediated by signaling pathways dependent on the adaptor protein MyD88. Curr Biol 2000;10:1139–42.
71. Jiang Z, Zamanian-Daryoush M, Nie H, et al. Poly(dI.dC)-induced Toll-like receptor 3 (TLR3)-mediated activation of NFkappa B and MAP kinase is through an interleukin-1 receptor-associated kinase (IRAK)-independent pathway employing the signaling components TLR3-TRAF6-TAK1-TAB2-PKR. J Biol Chem 2003;278: 16713–9.
72. Sweet MJ, Stacey KJ, Kakuda DK, Markovich D, Hume DA. IFN-gamma primes macrophage responses to bacterial DNA. J. Interferon Cytokine Res 1998;18:263–71.
73. Gao JJ, Zuvanich EG, Xue Q, et al. Cutting edge: bacterial DNA and LPS act in synergy in inducing nitric oxide production in RAW 264.7 macrophages. J Immunol 1999;163:4095–9.